ISSN: 0975 -8542

Journal of Global Pharma Technology

Available Online at: www.jgpt.co.in

RESEARCH ARTICLE

Mesoporous Silica and Zno@Sio$_2$ as Adsorbents for Crystal Violet Dye Removal from Aqueous Solutions

Alaa Faroq Omar, Sameer H. Kareem*

Department of Chemistry-College of Science for Women-University of Baghdad-Iraq.

***Corresponding Author: Sameer H. Kareem**

Abstract

Sol-gel method was used to prepare two samples of mesoporous Silica ($mSiO_2$) and zinc oxide-mesoporous silica ($ZnO@mSiO_2$) in the presence of HydroxycetylHydroxy ethyl Diamonium Chloride (dehyquart) surfactant as template. The two adsorbents prepared were characterized by nitrogen adsorption-desorption, XRD and AFM techniques. The results show that the $mSiO_2$ sample has a mesopores in the range 2- 8 nm with a high degree of ordering of the porous structure, while $Zn@SiO_2$ sample has pore distribution in the range 2-50 nm. The adsorption ability of the two adsorbents to removal of Crystal Violet (CV) dye from aqueous systems has been studied using a batch experiments method to measure the adsorption as a function of contact time and adsorbent dose at the temperature 293 K. Adsorption isotherms were fitted with the Langmuir, Freundlich, Temkin, and Dubinin-Radushkevich models and the results show a best fitted for the two adsorbents, and the adsorption processes were physical adsorption type. The kinetic data were analyzed and found to match well with pseudo-second order kinetic model.

Keywords: *Mesoporous silica, Crystal Violet, $Zn@SiO_2$, Adsorption isotherm.*

Introduction

The first mesoporous silica called MCM-41 was prepared in 1992 by Beck et al [1].Which shows a hexagonal arrangement of uniform mesopores having dimensions in the range of 15-100 Å and 700 m^2/g surface areas. A surfactant templating mechanism was proposed for the creation of these materials. In 1998, Stucky and co-workers [2, 3] discovered another mesoporous materials, designated as SBA-15 consisting of thermally stable thick walls and hexagonal mesopores (4-10 nm) which overcame the weak hydrothermal stability encountered by M41S materials. Aquino et al [4].

Prepared MCM-41 and sulfate containing MCM-41 by the hydrothermal method using cethyltrimethylamonium bromide as template and characterized by BET surface area, X-ray diffraction, infrared spectroscopy and thermogravimetry. The two samples were used as catalyst in the isopropanol dehydration, in a fixed bed continuous flow reactor. Tani et al [5].Made (ZnO)/ (SiO_2) composite nanoparticles by flame spray pyrolysis. The mixed-oxide primary particle size was smaller than that of pure oxides. The primary particles consisted of ZnO nano-crystals and amorphous SiO_2, as seen by high-resolution transmission electron microscopy and X-ray diffraction analysis. The composite particles exhibited an excellent thermal stability and little crystalline growth of ZnO (e.g., from 1.9 to2.2 nm). Adak et al [6].Used sodium dodecyl sulfate surfactant for the surface modification of neutral alumina. The surfactant-modified alumina was used for the removal of crystal violet (CV), from aquatic environment with ~99% efficiency when CV present even at a high concentration (200 ppm).

The kinetic studies showed that 1 h shaking time was sufficient to achieve the equilibrium, and the removal followed the second order kinetics. Wagner et al [7]. report on the synthesis and the gas-sensing properties of mesoporous zinc oxide using replication method for the synthesis of mesoporous SBA-15 silica which is utilized for synthesizing mesoporous carbon, which,

in turn, is employed for yet another replication step, using zinc nitrate as the precursor. The resulting material is characterized by X-ray diffraction and nitrogen physisorption and its gas-sensing properties are compared with a non-porous ZnO sample. In our laboratory, Ibrahim et al [8].Prepared mesoporous silica from sodium silicate as a precursor and cetyltrimethylammonium bromide as template by sol-gel method, and used as adsorbent for removes cetyldimethylbenzylammonium chloride from aqueous solution. The equilibrium data were best represented by the Freundlich isotherm model.

The results of kinetic investigation matched well with pseudo-second-order, while the results of thermodynamic study indicate that these systems were spontaneous and exothermic in nature. In the present work, sol-gel method was used to prepare mesoporous silica using locally sodium silicate as precursor and a surfactant as template. The adsorption ability of the prepared silica for CV removal was studied including the equilibrium, thermodynamic, kinetics, and adsorptions isotherms.

Materials and Methods

Chemicals

Sodium silicate (14% NaOH, 27% SiO_2) as silica precursor and HydroxyCetyl Hydroxyethyl Diamonium Chloride (Dehyquart E-CA) as template were purchased from local market. Methylene blue was purchased from Fluka.

Characterization

The prepared mesoporous silica was characterized by XRD, AFM and N_2 adsorption – desorption isotherms. The adsorption- desorption isotherms of N_2 at 77 K were obtained using a Micromeritics ASAP 2020 Instrument. The particle size and particle size distributions were analyzed using Atomic Force Microscopy (AFM) SPM-AA 3000, Advanced Angestrum Inc., and USA. The X-ray diffraction (XRD) patterns were obtained with a Rigaku diffractometer using Cu Kα (λ = 0.154 nm) radiation.

Preparation of Adsorbents

Preparation of $MSIO_2$

3.5 g of Hydroxy Cetyl Hydroxy ethyl Di methylamonium Chloride (dehyquart) was dissolve in 150 ml of distilled water and 3.5g of sodium silicate dissolved in 150 ml of distilled water was added to the mixture drop by drop from burette for 3 hour. The white precipitate formed was recovered by filtration, washed with water, after aging at 80 ˚C for one day. After drying at 80 °C the surfactant was removed by calcinations at 600 ˚C for 4 hours.

Preparation of ZnO

60 mL of 0.2 M zinc nitrate Zn $(NO_3)_2$ and (5.25) g of dehyquart dissolved in 225 ml distilled water were mixed and 45 ml of 0.4M sodium bicarbonate ($NaHCO_3$) was added to the mixture drop by drop from burette for 2h. The solution was aged in room temperature for one day; the precipitate formed was recovered by filtration and washed with distilled water. The precipitate was dried at 80˚C for 2h and calcinied at 600˚C for 3h.

Preparation of $ZnO@SiO_2$

1g from ZnO was suspended in around bottom flask contained 150 ml distilled water and 3.5 g of dehyquart by vigorously stirring. 3.5g of sodium silicate solution dissolved in 150 ml distilled water was added to the mixture drop by drop from burette for 3h. The solution was aged in room temperature for one day, and then the precipitate formed was recovered by filtration and washed with distilled water. The precipitate was dried at 80˚C for 2h and calcinied at 400˚C for 3h.

Adsorption Procedure

The adsorption isotherm was performed using 100 ml of different CV concentration (10, 15, 20, 25, 30, 35, 40 mg/L) with 0.03g and 0.035 g of $mSiO_2$ and ZnO-$mSiO_2$adsorbents respectively. The CV-$mSiO_2$ and CV- $ZnO@SiO_2$ mixture systems were shaken well for 60 min and 75 min respectively to reach equilibrium. A sample has been pipette and placed in the centrifuge for 10 minutes; the concentrations of the CV solution before and after the adsorption were determined by UV-Visible spectrophotometer at λ_{max} 590 nm. The amount of dye adsorbed was determined by the equation:

$$q_e = (C_0 - C_e)\, V/\, W \quad - - - - - - - (1)$$

Where q_e is the equilibrium adsorption capacity of CV adsorbed on unit mass of the adsorbent (mg /g), C_0 and C_e are the initial CV concentration (mg L^{-1}) and at equilibrium respectively, (L) is the volume of CV solution and W (g) is the weight of adsorbent.

The concentration of CV was measured and the percentage removal (R %) was determined according to the equation :

$$R\% = (C_0 - C_e) \times 100 / C_0 \quad - - - - - - - (2)$$

Results and Discussion

Characterization of Adsorbents

The small-angle XRD data (Fig. 1) shows that both $mSiO_2$ and $ZnO@mSiO_2$ samples present ordered mesopore, with at least one low-angle (100) Bragg reflection. The most ordered material is $mSiO_2$which presenting three (100), (110) and (200) Bragg reflections characteristic for two-dimensional hexagonal [9]. Using the data obtained and Scherer equation ($D = 0.9\ \lambda / B \cos \theta$), where λ is wavelength of x-ray (Å), B is FWHM (radian) and θ is position (radian), the crystalline size for $mSiO_2$ and $ZnO@mSiO_2$ are 45.06 nm and 20.11 nm respectively. The mesoporous structure of the two samples was also characterized by typical N_2 adsorption–desorption technique. The isotherm of $mSiO_2$ (Fig. 2) exhibits the typical IV with hysteresis loop of type H2, which indicates that the ink bottle-type mesopores are present. The isotherm of $ZnO@mSiO_2$ shows ameso- and microspores (Fig. 3). According to the BJH method calculation of the desorption branch of N_2 isotherm, the average mesopore sizes (d_{BJH}) of $mSiO_2$ and $ZnO@mSiO_2$ were 2.61 nm and 7.99 nm respectively. The texture properties of the two samples were listed in Table (1).

Table 1: The texture properties of the two adsorbents

Sample	$S_{BET}(m^2g^{-1})$	V_P (cm^3g^{-1})	d_{BJH} (nm)
$mSiO_2$	1164.31	1.068	2.61
$Zn@mSiO_2$	18.34	0.038	7.99

The Histogram of Granularity Distribution for a) $mSiO_2$ and b) $ZnO@mSiO_2$ obtained from atomic force microscopy is shown in Fig. 4. The figure shows that the diameter of the particles are in the range55-125nm and average diameter of particles 68.68nm for $mSiO_2$ sample, while for $ZnO@mSiO_2$ sample the figure shows that the particles in range 90-190 nm, and average diameter of particles 112.32nm. Comparing the results, one can see that the granule size of $ZnO@mSiO_2$ is larger than the granule size of $mSiO_2$.

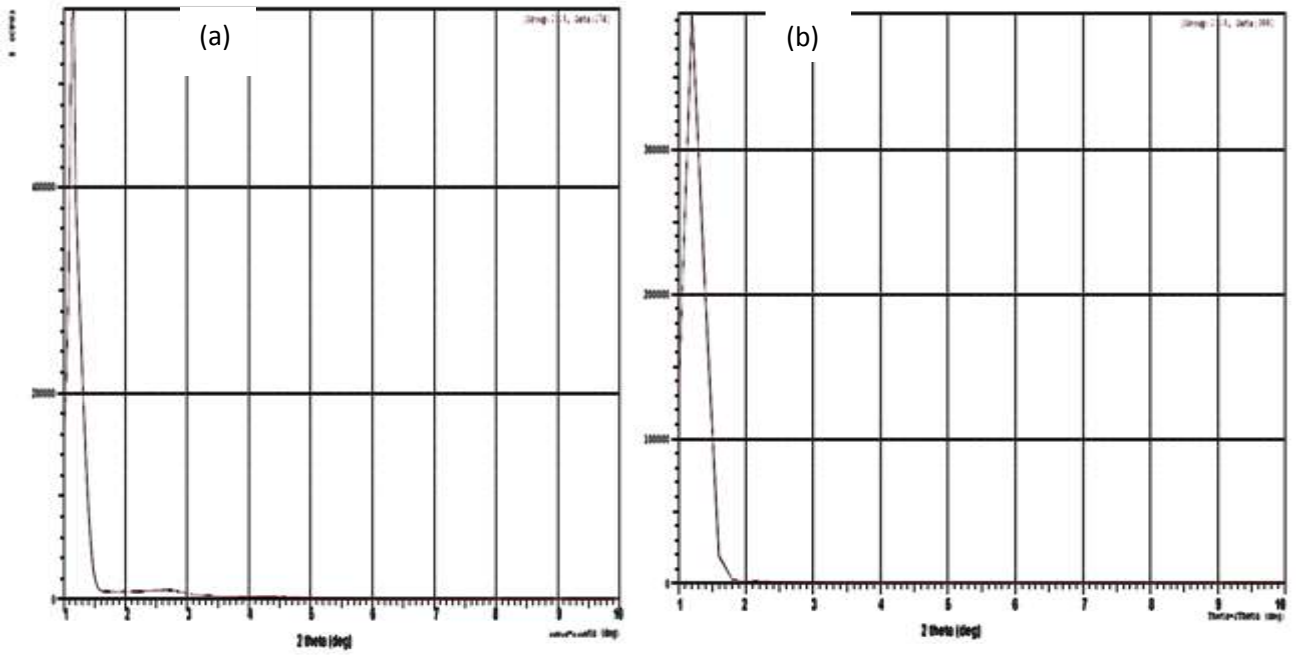

Figure1: XRD Patterns of (a) $mSiO_2$ (d) $ZnO@mSiO_2$ after calcinations in 2θ range (0-10)

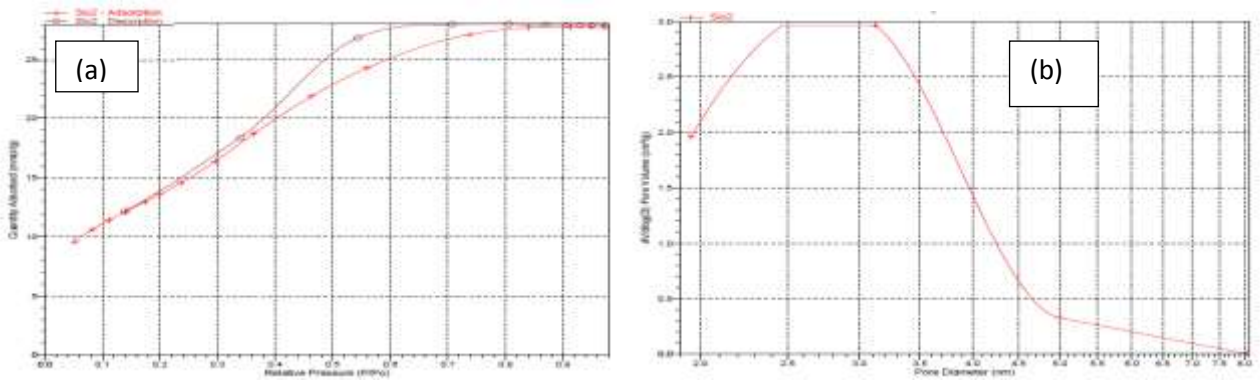

Figure 2: a) N_2 adsorption-desorption isotherm b) PZD for $mSiO_2$.

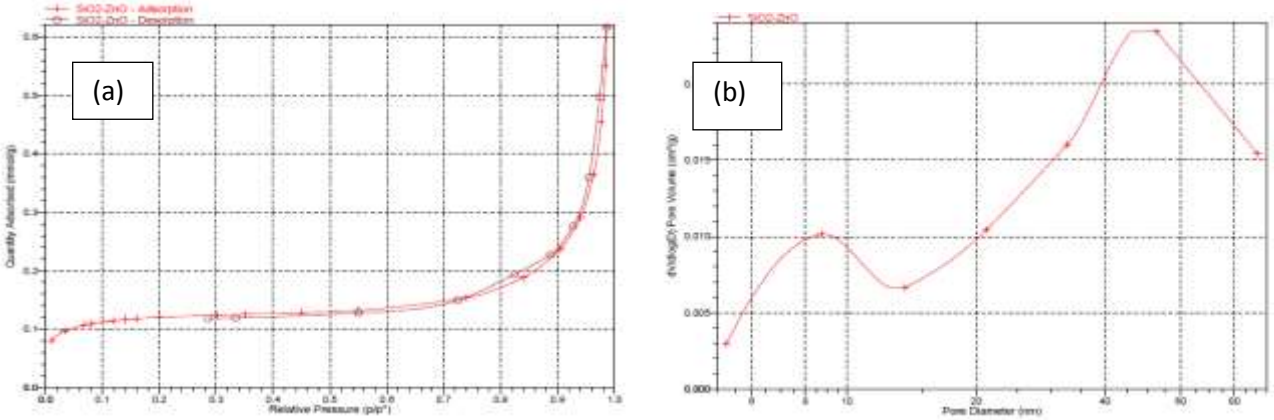

Figure 3: a) N_2 adsorption-desorption isotherm b) PZD for $ZnO@SiO_2$

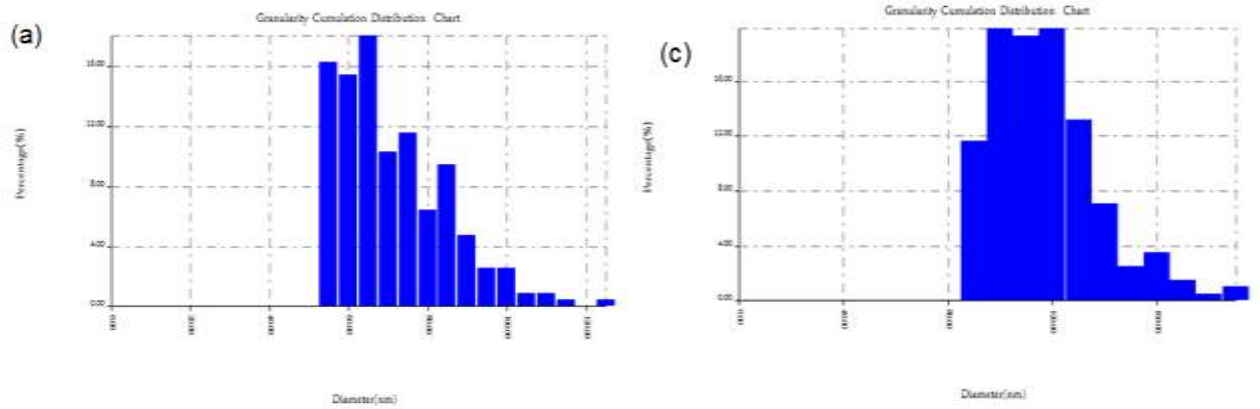

Figure 4: Histogram of Granularity Distribution for (a) $mSiO_2$ and (b) $ZnO@mSiO_2$

Adsorption Behavior

Effect of Contact Time and Adsorbent Dose

The effect of contact time between CV with $mSiO_2$ and $ZnO@mSiO_2$ was studied for solutions in which the concentration was 20 mg L^{-1}. We observed the adsorption of a satisfactory amount of CV onto the $mSiO_2$ and $ZnO@mSiO_2$ after 60 and 75 min respectively (Fig. 5). Fig. 5 shows that the quantity of the removal of the CV dye increased with increase in the dose of the adsorbent. This may be due to the availability of surface active sites resulting from the increased dose and conglomeration of the adsorbent. The increase in the number of removal of CV is found to be meager after a dose of 0.03 g and 0.035g for $mSiO_2$ and $ZnO@mSiO_2$ respectively. Therefore, they are fixed as optimum dose of adsorbent for further studies.

Adsorption Isotherms

In the present study, three adsorption isotherm models (Langmuir, Freundlich, and Temkin) have been used to study the adsorption capacity and equilibrium coefficients for adsorption of CV on the two samples. These models are:

$$q_e = \frac{q_m K_L C_e}{(1 + K_L C_e)} \quad \text{------- (3)}$$

$$q_e = (C_e)^{1\backslash n} \quad \text{------- (4)}$$

$$q_e = B\ Ln\ (K_t\ C_e) \quad \text{-------- (5)}$$

Where q_m is Langmiur constant related to the capacity and K_L is related to the energy of adsorption, n and K_f are Freundlich constants related to the intensity of adsorption and adsorption capacity respectively, B and K_T the Temkin isotherm constants. These isotherms are fitted employing the non- linear fitting method using the software called (STATISTICA Module Switcher). Fig. 6 presents how well the three equations fit experimental data for $mSiO_2$ and $ZnO@mSiO_2$ – CV systems at 293 K and the parameters of the three isotherms for the two systems studied are shown in Table 2.

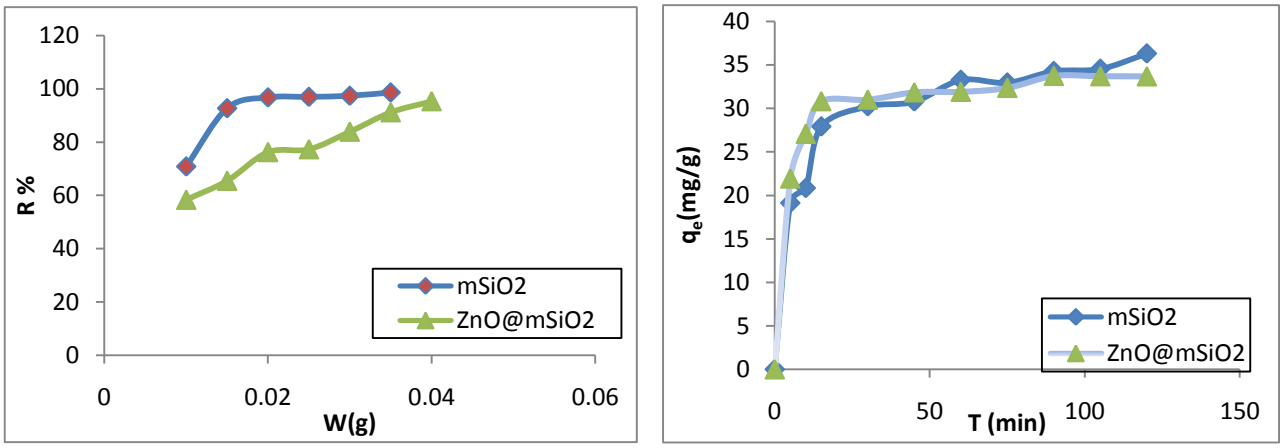

Figure 5: a) The effect of adsorbent dose and b) contact time for CV adsorption on the two adsorbents (C_o =20 mg/L, T=293 K)

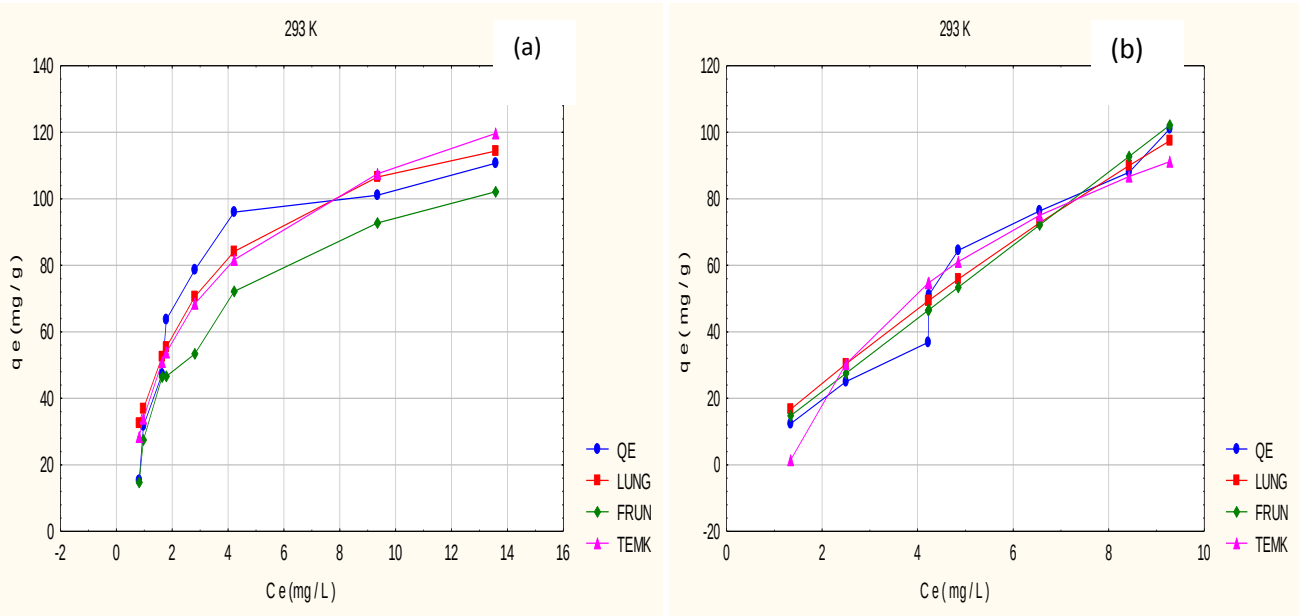

Figure 6: Adsorption isotherm analysis of; a) CV-$mSiO_2$ b) CV-$ZnO@SiO_2$ systems at 293 K

Table 2: The parameters of Langmuir, Frendlich and Temkin models for adsorption of CV on $mSiO_2$ and $ZnO@SiO_2$ at 293K

Adsorbent	Lungmuir model				Freundlich model			Temkin model		
	Q_m	K_L	R_L	R^2	n	K_F	R^2	B	K_T	R^2
$mSiO_2$	136.42	0.38	0.07	0.97	2.50	42.50	0.93	74.84	3.02	0.95
$ZnO@mSiO_2$	1449.66	0.008	0.74	0.98	1.03	11.52	0.98	106.78	0.76	0.95

As seen from the Fig (9), and the results of correlation coefficient (R^2) Table (2), indicate that the experimental data fitted well to the three adsorption models Langmuir, Freundlich and Temkin. Dubinin-

Radushkevich isotherm [10] which can be written as:

$$\mathrm{Ln}q_e = \ln q_m - \beta\varepsilon^2 \quad \ldots\ldots (6)$$

Was used to predict the nature of adsorption process through the determination of the mean adsorption energy (E) using equation [11]:

$$E = 1/\beta^{1/2} \quad - - - - - - - (7)$$

Where ε is the Polanyi potential which equal:

$$\varepsilon = (1+1/C_e) \quad \ldots\ldots\ldots (8)$$

And β is a constant related to the adsorption energy ($mol^2\ kJ^{-2}$).

The calculated mean adsorption energy E for the adsorption on the two adsorbents $mSiO_2$ and $ZnO@mSiO_2$ are 2.82 and 2.00 kJ/mol respectively which reveals that these adsorption processes were dominated physical adsorption since all values of E are less than 8kJmol^{-1}[12].

Kinetics Study

Three kinetic models (Lagergren-first-order [13, 14], pseudo-second order [15], and Intra-particle diffusion [16] are used to study the adsorption kinetic behavior of CV (20 mg/L) onto the two adsorbents. The equations are as follows:

$$\ln q_e - q_t = ln q_e - k_1 t \quad - - - - - - - (9)$$

$$t/\ = 1/(k_2 q_e^2) + (1/q_e)\, t \quad - - - - - - - (10)$$

$$q_e = k_d\, t^{1/2} + C \quad - - - - - - - (11)$$

Where k_1 (min^{-1}), k_2 (g mg^{-1} min^{-1}), and k_d (mg g^{-1} min$^{-1/2}$) are the rate constants of the pseudo-first order, pseudo-second order, and intra-particle diffusion kinetics respectively. q_e and q_t are the amounts of CV adsorbed on the surface of the adsorbent at equilibrium and at any time (mg g^{-1}) respectively, C is constant. The kinetics parameters obtained from slope and intercept of the plots in Figures (7) and (8) are shown in Table (3).

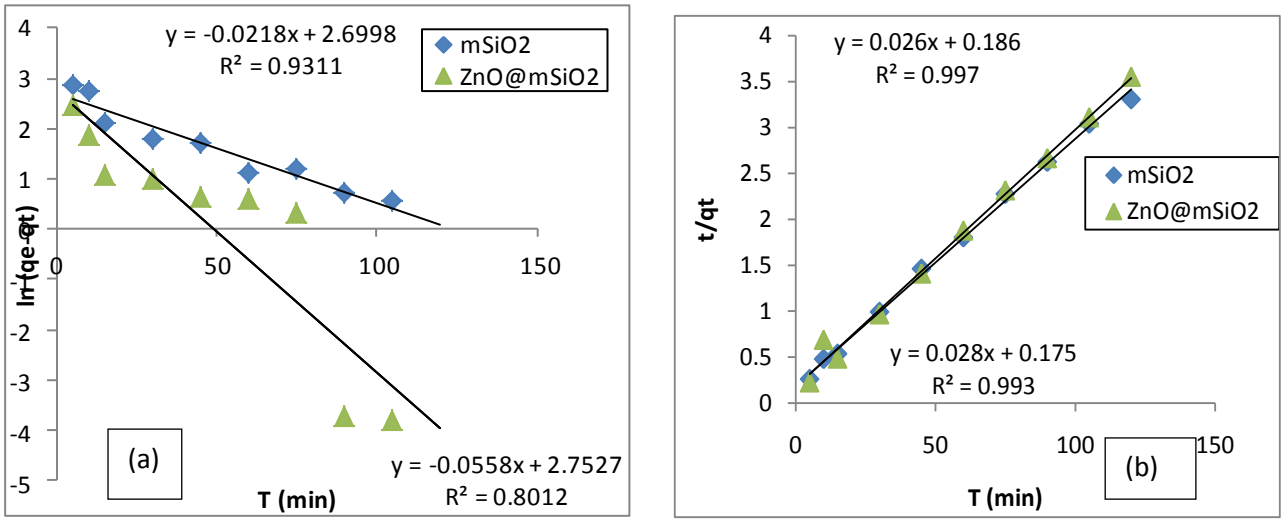

Figure 7: a) The pseudo- first order kinetic (b) the pseudo- second order kinetic at (C_o = 20 mg/L and 293 K)

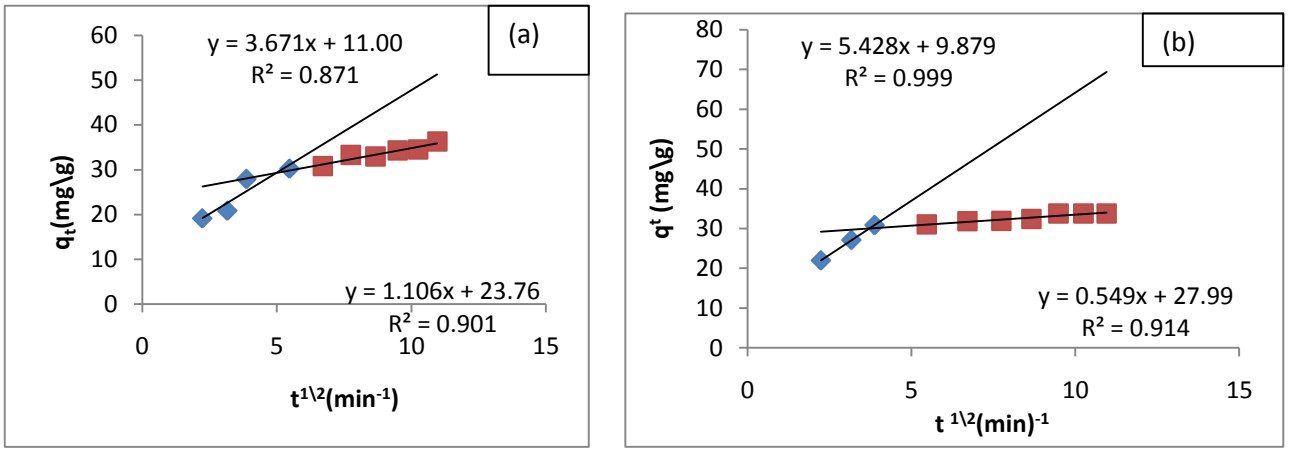

Figure 8: The intra-particle diffusion model for the adsorption of CV on (a) $mSiO_2$ and (b) $ZnO@mSiO_2$ at (C_o = 20 mg/L and 293 K)

Table 3: Kinetic parameters for adsorption of CV on $mSiO_2$ and $ZnO@mSiO_2$ at C_O =20 mg/L and 293 K

Model	Parameters	$MSIO_2$	$ZnO@mSiO_2$
Pseudo first order	q_e (mg/g)	14.87	15.67
	k_1 (min^{-1})	0.021	0.055
	R^2	0.93	0.80
Pseudo second order	q_e (mg/g)	37.17	35.71
	k_2(g (mg min)$^{-1}$)	0.003	0.003
	h(mg $g^{-1}min^{-1}$)	5.37	4.96
	R^2	0.99	0.99
Diffusion model	k_{d1} (mg g^{-1} $min^{-1/2}$)	3.67	5.42
	R^2	0.87	0.99
	k_{d2} (mg g^{-1} $min^{-1/2}$)	1.10	0.54
	R^2	0.90	0.91

From the correlation coefficient (R^2) values presented in Table (3), it can be seen that the adsorption perfectly complies with pseudo-second order model. Also, it can be seen from the plot of intra-particle diffusion model, the adsorption was controlled by two stages. The first linear portion was a gradual adsorption where intraparticle diffusion was the rate determining factor. The second linear portion was the equilibrium stage due to low concentration of dye in the solution phase. As can be seen in the plot, the intraparticle diffusion was not the rate determining factor as the first linear portion of the plot did not pass through the origin [17, 18].

Conclusions

The foregoing results of this study confirm the presence of mesoporosity in the samples prepared and have a narrow pore size distribution and indicates that the $mSiO_2$ adsorbent is quite based on its highest BET surface area of 1164.31m^2/g. Adsorption isotherm data fitted quite well to various concentration ranges under study for Langmuir, Freundlich and Temkin models indicating that CV dye has very good affinity towards adsorbents prepared. Kinetics of adsorption was better explained by pseudo-second-order kinetics.

References

1. Beck JS, Vartuli JC, Roth WJ, Leonowicz ME, Kresge CT, Schmitt KD, Higgins JB (1992) A new family of mesoporous molecular sieves prepared with liquid crystal templates. Journal of the American Chemical Society, 114(27): 10834-10843.
2. Zhao D, J Feng, Q Huo, N Melosh, GH Fredrickson, BF Chmelka, GD Stucky (1998) Tri block Copolymer Syntheses of Mesoporous Silica with Periodic 50 to 300 Angstrom Pores. Science, 279: 548-552.
3. Zhao D, Q Huo, J Feng, BF Chmelka, GD Stucky (1998) Nonionic Triblock and Star Diblock Copolymer and Oligomeric Surfactant Syntheses of Highly Ordered, Hydrothermally Stable, Mesoporous Silica Structures. J. Am. Chem. Soc., 120: 6024-6036.
4. Aquino JM, Souza CD, Araujo AS (2001) Synthesis and characterization of sulfate-supported MCM-41 material. International Journal of Inorganic Materials, 3(6): 467-470.

5. Tani T, Mädler L, Pratsinis SE (2002) Synthesis of zinc oxide/silica composite nanoparticles by flame sprays pyrolysis. Journal of materials science, 37(21): 4627-4632.
6. Adak A, Bandyopadhyay M, Pal A (2005) Removal of crystal violet dye from wastewater by surfactant-modified alumina. Separation and Purification Technology, 44(2):139-144.
7. Wagner T, Waitz T, Roggenbuck J, Fröba M, Kohl CD, Tiemann M (2007) Ordered mesoporous ZnO for gas sensing. Thin Solid Films, 515(23):8360-8363.
8. Ibrahim Q, Ali IH, Kareem SH (2016) Removal of Cetyldimethylbenzyl ammonium Chloride Surfactant from Aqueous Solution by Adsorption onto Mesoporous Silica. International Journal of Science and Research, 5(12); 1536-1542.
9. Marilena P, R-A Mitran, Ana-Maria LC, Matei DB (2015) Mesoporous ceria-silica composites as carriers for doxycycline. U.P.B. Sci. Bull., Series B, 77(3): 13-24.
10. MM Dubinin (1960) The Potential Theory of Adsorption of Gases and Vapors for Adsorbents with Energetically Nonuniform Surfaces. Chem. Rev., 60(2):235-241.
11. Nunes Cleiton A, Guerreiro Mário C (2011) Estimation of surface area and pore volume of activated carbons by methylene blue and iodine numbers. Quim. Nova,34(3): 472-476.
12. Chowdhury S, Chakraborty S, Saha P (2011) Biosorption of Basic Green 4 from aqueous solution by *Ananas comosus* (pineapple) leaf powder. Colloids Surf B Bio interfaces, 84: 520-527.
13. Tseng RL, Wu FC, Juang RS (2003) Liquid-phase adsorption of Dyes and Phenols using Pinewood Based Activated Carbons. Carbon, 41: 487-495.
14. Lagergren S (1898) About the theory of so-called adsorption of soluble substances. K Sven Vetenskapsakad Handl, 24: 1-39.
15. Chiou MS, Li HY (2003) Adsorption Behaviour of Reactive Dye in Aqueous Solutions on Chemical Cross Linked Chitosan Beads. Chemosphere, 50: 1095-1105.
16. Weber WJ, JC Morris (1963) Kinetics of Adsorption on Carbon from Solution J. San. Eng. Div. ASCE, 89: 31-60.
17. Nihar RB, P Santanu (2010) Effect of Electrolyte Solutions on the Adsorption of Surfactants at PTFE-Water Interface. Ind. Eng. Chem. Res. 49(15): 7060-7067.
18. Abdul Salam J, N Das (2013) Biosorptive Removal of Lindane Using Pretreated Dried Yeast Cintractia Sorghi Vitjzn02-Equilibrium and Kinetic Studies. International Journal of Pharmacy and Pharmaceutical Sciences, 5(3): 987-993.

